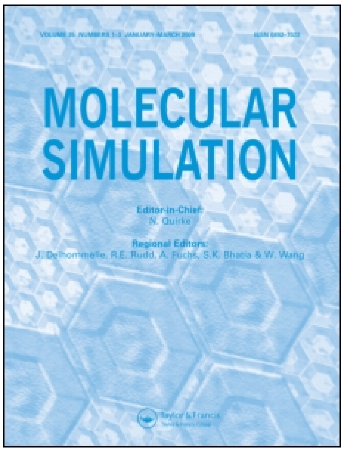

Molecular Simulation
Publication details, including instructions for authors and subscription information:
http://www.informaworld.com/smpp/title~content=t713644482

A Computational Investigation of the Dynamics of Urea Molecules in Solids

Stephanie Camus[a]; Kenneth D. M. Harris[a]; Sarah L. Price[b]
[a] School of Chemistry, University of Birmingham, Birmingham, U.K. [b] Department of Chemistry, University College London, London, U.K.

To cite this Article Camus, Stephanie , Harris, Kenneth D. M. and Price, Sarah L.(1996) 'A Computational Investigation of the Dynamics of Urea Molecules in Solids', Molecular Simulation, 18: 5, 303 — 323

To link to this Article: DOI: 10.1080/08927029608024126

URL: http://dx.doi.org/10.1080/08927029608024126

Molecular Simulation, 1996, Vol. 18, pp. 303-323
Reprints available directly from the publisher
Photocopying permitted by license only

A COMPUTATIONAL INVESTIGATION OF THE DYNAMICS OF UREA MOLECULES IN SOLIDS

STEPHANIE CAMUS[1], KENNETH D. M. HARRIS[1]*,
SARAH L. PRICE[2]

[1]*School of Chemistry, University of Birmingham, Edgbaston,
Birmingham B15 2TT, U.K.*
[2]*Department of Chemistry, University College London, 20 Gordon Street,
London WC1H OAJ, U.K.*

(Received June 1996, accepted July 1996)

A computational investigation of the dynamic properties of urea molecules in the pure crystalline phase of urea and in the urea tunnel structure (which is found in the conventional urea inclusion compounds) is reported. Both of these crystalline solids are extensively hydrogen bonded structures, and in both cases it has been shown experimentally that the urea molecules undergo 180° jumps about their C=O bonds at sufficiently high temperature. The computational investigations reported here have probed aspects of the potential energy barriers for this reorientational motion, and the possibility of correlations between the motions of different urea molecules. Various structural models representing clusters of urea molecules in these solids were considered, with two different potential energy parameterizations used to compute the energies of these clusters. The energetic and structural properties of the clusters were investigated as a function of rotation of a reference urea molecule, leading to new insights concerning the degree of correlation between the rotational motions of different urea molecules. A critical assessment is presented of the extent to which the results from these computational investigations can be compared with experimental results on the dynamic properties of the urea molecules.

Keywords: Urea; reorientational motions; clusters

1. INTRODUCTION

In this paper, we consider the dynamic properties of urea molecules in the pure crystalline phase of urea [1,2] and in the urea tunnel structure [3,4] which is

---

*Author to whom all correspondence should be addressed.

found in the conventional urea inclusion compounds [5–8]. In these urea inclusion compounds, the tunnels of the urea "host" structure are filled with a dense packing of "guest" molecules; examples of suitable guest molecules are *n*-alkanes and α,ω-disubstituted *n*-alkanes. Both the pure urea structure and the urea tunnel structure are extensively hydrogen bonded networks; in both networks, each urea molecule is involved in a total of eight intermolecular hydrogen bonds involving six nearest neighbour urea molecules, but the two networks differ in terms of the connectivity of a given urea molecules to its six nearest neighbours.

It has been shown using a variety of experimental techniques that, at sufficiently high temperature, the urea molecules in the pure urea structure and the urea tunnel structure undergo 180° jumps about their C=O bonds. Specifically, for the pure crystalline phase of urea, the 180° jump motion has been investigated by ^{1}H NMR spectroscopy [9], ^{2}H NMR spectroscopy [10], and ^{14}N NQR spectroscopy [11], leading to estimated activation energies of 38 kJ mol^{-1} [9], (46 ± 8) kJ mol^{-1} [10] and (49 ± 8) kJ mol^{-1} [11]. For pure crystalline urea, it has also been suggested [9, 10, 12] that the NH_2 groups rotate about the C—N bonds, with activation energy estimated to be (63 ± 13) kJ mol^{-1} [10] and 51 kJ mol^{-1} [12]. For the nonadecane/urea [13] and α, ω-dibromoalkane/urea [14] inclusion compounds, the 180° jump motion of the urea molecules about their C=O bonds has been investigated by ^{2}H NMR spectroscopy, with the activation energy estimated to be (23 ± 2) kJ mol^{-1} for *n*-nonadecane/urea [13]. Clearly the 180° jump motion of the urea molecules about their C=O bonds implies breakage of hydrogen bonds, although the experimental techniques employed are unable to indicate whether the 180° jumps of different urea molecules are correlated to one another.

For *n*-alkane/urea and α,ω-dibromoalkane/urea inclusion compounds, incoherent quasielastic neutron scattering has shown [15, 16] that, above the low-temperature phase transitions for these materials, the n-alkane and α, ω-dibromoalkane guest molecules undergo both translation along the tunnel and rotation about the tunnel axis on the picosecond timescale. However, no motion of the urea molecules could be detected on this timescale by incoherent quasielastic neutron scattering [17], leading to the conclusion that the 180° jump motion of the urea molecules is not correlated with these rotational and translational motions of the guest molecules.

In this paper, we report a computational investigation of the dynamics of urea molecules in the pure urea structure and the urea tunnel structure. Important considerations include whether the 180° jump motions of different urea molecules are correlated with one another, and an assessment of the ability of different potential energy parameterizations to model structural and dynamic properties of these solids. This represents a first step in our computational investigation of the dynamics of urea molecules in these materials.

2. COMPUTATIONAL ASPECTS

2.1. Description of Models and Methodology

Both the pure crystalline phase of urea and the urea tunnel structure were represented by "clusters" comprising a central urea molecule surrounded by shells of neighbouring molecules. Two different potential energy parameterizations, discussed in Section 2.2, were considered and compared. To investigate the dynamic properties, the total energy of the cluster was minimized with respect to variation of selected geometric variables (*vide infra*). It is important to note that an alternative possibility would have been to represent the structures using periodic boundary conditions; however, this approach is inappropriate as it will impose correlated motions on the system (molecules related by the periodicity of the replicating unit are constrained to behave identically). However, when considering a cluster model it is important that the cluster is sufficiently large to ensure that the properties of the cluster represent those of the bulk crystal structure.

Clusters representing the pure urea structure were constructed using fractional coordinates determined [18] from neutron diffraction data (recorded at 293 K). The centre of mass of a reference urea molecule was chosen as the origin of the Cartesian reference frame, with the z-axis lying along the C=O bond and the xz-plane parallel to the plane of this urea molecule. This molecule centred at the origin of the Cartesian reference frame is subsequently called the central urea molecule, and is denoted by $i = 0$.

The urea tunnel structure was constructed using fractional coordinates of the carbon, nitrogen and oxygen atoms determined from X-ray diffraction data for hexadecane/urea [4], with the hydrogen atoms added in positions calculated from the N—H bond lengths and C—N—H and H—N—H bond angles reported [18] from neutron diffraction data for the pure crystalline phase of urea. The centre of mass of a reference urea molecule was chosen as the origin of the Cartesian reference frame, with the z-axis lying along the C=O bond of this urea molecule and the y-axis parallel to the tunnel axis. Note that the normal to the plane of each urea molecule forms an angle of 81.5° with respect to the direction of the tunnel axis (y-axis). The molecule centred at the origin of the Cartesian reference frame is subsequently called the central urea molecule, and is denoted by $i = 0$.

In each structure, it is convenient to define the position of each urea molecule (labelled i) by the position vector of the centre of mass relative to the origin of the Cartesian reference frame, and to define the orientation of each urea molecule relative to the orientation of the central urea molecule in the experimental crystal structure by a set of Euler angles $\{\alpha_i, \beta_i, \gamma_i\}$. Rotation of urea molecule i about its C=O bond is represented by variation of the Euler angle γ_i. This is the only geometric parameter that was varied in the energy minimization calculations reported here. The molecules were rigid, and the positions of their centres of mass and the orientations of their C=O bonds were fixed at the values observed in the experimental crystal structures for the pure urea structure and the urea tunnel structure.

The clusters considered in this work are specified in Table I for the pure urea structure (see also Fig. 1) and the urea tunnel structure (see also Fig. 2). The clusters used in models of types P1 (P represents the pure urea structure) and T1 (T represents the urea tunnel structure) comprise the central urea molecule surrounded by the urea molecules directly hydrogen bonded to it (this is called the first shell of urea molecules). In models of types P2 and T2, the molecules directly hydrogen bonded to each molecule of the first shell are also considered (these represent the second shell of urea molecules). In model P3, two urea molecules of the third shell (i.e. directly hydrogen bonded to molecules of the second shell but not directly hydrogen bonded to molecules of the first shell or

TABLE I Definition of models considered for the pure urea structure and the urea tunnel structure (P denotes the pure urea structure; T denotes the urea tunnel structure)

models	*molecules considered*	*variables*
P1A/T1A	central molecule ($i = 0$) first shell ($i = 1 - 6$)	γ_0
P1B/T1B	central molecule ($i = 0$) first shell ($i = 1 - 6$)	γ_i; $i = 0, \ldots, 6$
P2A/T2A	central molecule ($i = 0$) first shell ($i = 1 - 6$) second shell ($i = 7 - 24$ for P2A; $i = 7 - 26$ for T2A)	γ_0
P2B/T2B	central molecule ($i = 0$) first shell ($i = 1 - 6$) second shell ($i = 7 - 24$ for P2B; $i = 7 - 26$ for T2B)	γ_i; $i = 0, \ldots, 6$
P2C	central molecule ($i = 0$) first shell ($i = 1 - 6$) second shell ($i = 7 - 24$)	γ_i; $i = 0, \ldots, 24$
P3	central molecule ($i = 0$) first shell ($i = 1 - 6$) second shell ($i = 7 - 24$) 2 molecules of third shell ($i = 25, 26$)	γ_i; $i = 0, \ldots, 6, 15, 16$

the central urea molecule) are included in addition to the molecules in the models of type P2.

It is important to note that the tunnels of the urea tunnel structure are "empty"; this represents a hypothetical (but nevertheless interesting) situation as, in practice, the urea tunnel structure exists only when the tunnels contain a dense packing of guest molecules (see also the discussion in Section 4).

The ORIENT program [19] was used to calculate energetic properties of the clusters of urea molecules by minimizing the total energy of the cluster with respect to selected geometric variables (the rotation angles (γ_i) of all, or a subset of, the non-central urea molecules). The dynamic properties were investigated by rotating the central urea molecule about its C═O bond (i.e. variation of γ_o), usually in steps of $\Delta\gamma_o = 10^\circ$ or 5°; at each step, the rotation angle (γ_o) of the central urea molecule was fixed and the neighbouring molecules (or a subset of the neighbouring molecules) were allowed to reorient about their C═O bonds (i.e. relaxation of their Euler angles γ_i) in order to minimize the total energy of the cluster. The "configuration" of the system is specified by the set of rotation angles $\{\gamma_i;\ i = 0, 1, 2, \ldots, n\}$. In general, the initial configuration used for structural relaxation with a given value of γ_o (e.g. $\gamma_o = \phi$) was taken as the optimum configuration of the non-central urea molecules (i.e. $\{\gamma_i;\ i = 1, 2, \ldots, n\}$) obtained for the *previous* value of γ_0 (i.e. $\gamma_o = \phi - \Delta\gamma_o$). In this way, the total energy and the optimum configuration of the clusters were determined as a function of the rotation angle γ_o of the central urea molecule. It should be noted that the results of such calculations may depend upon the choice of $\Delta\gamma_o$.

2.2. Potential Energy Parameterizations

2.2.1. Hagler-Huler-Lifson (HHL) potential

The potential of Hagler, Huler and Lifson (specified in Tab. IV of ref. 20) includes repulsion and dispersion terms (Lennard-Jones (6, 12) potential) and the electrostatic contribution is represented by point charges located on each atomic site. [Note that, in this potential, there are no repulsion and dispersion terms for the hydrogen atoms of the urea molecule, and atom-atom interactions involving these atoms contribute only to the electrostatic energy]. This potential was developed by optimizing the bulk crystal structures and energetic properties of a series of amides, including the pure crystalline phase of urea. The structure obtained following energy minimization of the pure urea structure using the HHL potential is in good agreement ($\Delta a = -0.08$ Å

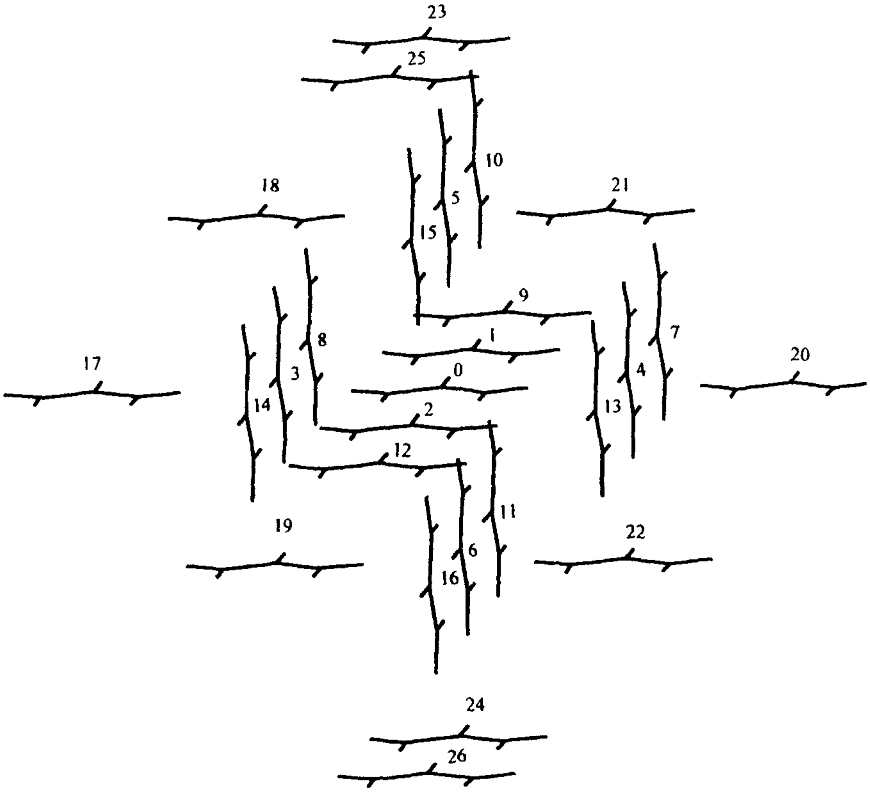

FIGURE 1 Specification of the molecules considered in the clusters representing the pure urea structure (as indicated in Tab. I, model P3 comprises all the molecules show, whereas other models comprise a subset of these molecules). The configuration ($\gamma_i = 0°: i = 0,\ldots, 26$) shown represents the geometry of the corresponding cluster in the experimental crystal structure.

$[(\Delta a)/a \approx -0.01]$; $\Delta c = 0.03$ Å $[(\Delta c)/c \approx 0.006]$) with the experimental crystal structure.

2.2.2. *Williams-Cox-Mitchell-Price (WCMP) potential*

In this potential, the distributed multipole description (*vide infra*) [21, 22] of the molecular charge distribution is combined with a modified version [23] of the potential of Williams and Cox (which includes dispersion and exponential repulsion terms). The parameters for the C...C and N...N interactions were taken from the work of Williams and Cox on azahydrocarbons [24], the parameters for O...O interactions were taken from the work of Williams and

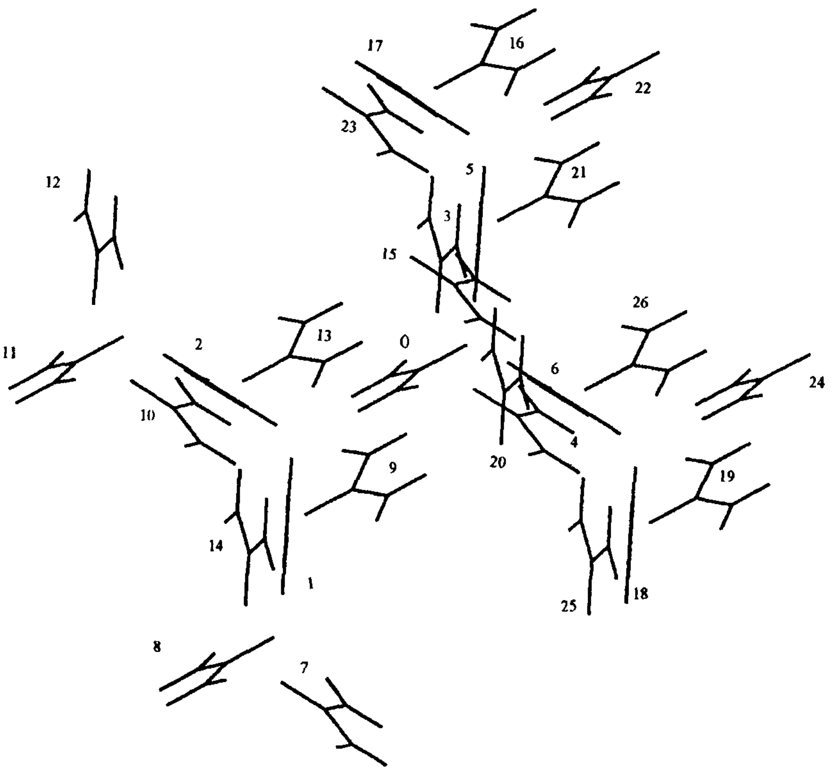

FIGURE 2 Specification of molecules considered in the clusters representing the urea tunnel structure (as indicated in Tab. I, models of type T2 comprise all the molecules shown, whereas other models comprise a subset of these molecules). The configuration $\{\gamma_i = 0°: i = 0, 1, \ldots, 26\}$ shown represents the geometry of the corresponding cluster in the experimental crystal structure.

Cox on oxohydrocarbons [25], and the parameters for H...O interactions were taken from the work of Mitchell and Price [26]. Parameters for interactions between other atom types were determined using the following combinations laws: $A_{ij} = (A_{ii}A_{jj})^{1/2}$; $B_{ij} = (B_{ii} + B_{jj})/2$; $C_{ij} = (C_{ii}C_{jj})^{1/2}$. Parameters relating to the repulsion and dispersion terms in the WCMP potential used in this work are specified in Table II.

The charge distribution of the urea molecule was derived from a Distributed Multipole Analysis (DMA) of the SCF wavefunction determined from *ab initio* calculations (6–31G** basis set) using the program suite CADPAC [27]; the molecular charge distribution was represented by sets of multipoles (including terms up to rank 4) positioned on each atom of the urea molecule (the SCF wavefunction was calculated for isolated molecules having the same geometry

TABLE II Parameters relating to the repulsion [Aexp(– Br)] and dispersion [– C/r^6] terms used in the WCMP potential. Parameters for interactions denoted * were calculated, from the parameters for N...N, C...C, O...O and O...H interactions, using the combination laws: $A_{ij}=(A_{ii}A_{jj})^{1/2}$; $B_{ij}=(B_{ii}+B_{jj})/2$ $C_{ij}=(C_{ii}C_{jj})^{1/2}$

interaction	*A/kJ mol^{-1}*	*B/Å^{-1}*	*C/kJ mol^{-1}Å^6*	*reference*
N...N	254529	3.78	1378.4	24
N...C	306774.047	3.69	1833.85395	*
N...O	241987.584	3.87	1244.49066	*
N...H	42262.3964	4.22	150.189907	*
C...C	369743	3.60	2439.8	24
C...O	291658.36	3.78	1655.698	*
C...H	50937.2464	4.13	199.815986	*
O...O	230064.123	3.96	1123.5904	25
O...H	40180	4.31	135.5992	26
H...H	7017.31492	4.66	16.3646317	*

as the molecules in the pure urea structure and the urea tunnel structure). It has been shown [28] that SCF wavefunctions do not always reproduce the electrostatic contribution to the intermolecular potential and, in particular, do not always give a reliable estimate of the molecular dipole moment. For this reason, the values of the multipoles obtained from the SCF wavefunction were scaled such that the calculated dipole moment matches the experimental dipole moment. The dipole moment of the urea molecule obtained from SCF calculation (6–31G* basis set) is 5.08 D, whereas the experimental dipole moment of the urea molecule in the gas phase is reported [29] to be 3.8 D. The multipoles obtained from the DMA were scaled in order to reproduce this experimental dipole moment using the scaling factor (3.8 D)/(5.08 D) = 0.747.

The structure obtained following energy minimization of the pure urea structure using the WCMP potential is in good agreement ($\Delta a = -0.02$ Å [$(\Delta a)/a \approx -0.003$]; $\Delta c = 0.18$ Å [$(\Delta c)/c \approx 0.04$]) with the experimental crystal structure.

3. RESULTS

In this Section, we describe and discuss the results of our calculations on the pure urea structure and the urea tunnel structure; selected results from all these calculations are summarized in Table III. In Section 4, we discuss in detail the conclusions and implications of the results described here, as well as presenting

TABLE III Summary of results from graphs of $E(\gamma_0)$ *versus* γ_0 and graphs of γ_i *versus* γ_0 for the pure urea structure and the urea tunnel structure using the HHL and WCMP potentials. For all calculations, the step size for variation of γ_0 was $\Delta\gamma_0 = 10^\circ$, except models T1B and T2B for the WCMP potential, for which $\Delta\gamma_0 = 5^\circ$ was used. Notation: ΔE = rotation barrier; $_{E}\Delta\gamma_0$ = periodicity in γ_0 for graphs of $E(\gamma_0)$ *versus* γ_0; γ_0^{min} = value(s) of γ_0 corresponding to minima in $E(\gamma_0)$; γ_0^{max} = value(s) of γ_0 corresponding to maxima in $E(\gamma_0)$; $_{\gamma}\Delta\gamma_0$ = periodicity in γ_0 for graphs of γ_i *versus* γ_0; $_{max}\Delta\gamma_i$ = maximum fluctuation in any of the angles $\gamma_i\,(i \neq 0)$ for γ_0 varied from 0° to 360°

model		*HHL*	*WCMP*
P1A	ΔE/kJ mol^{-1}	21	12
	$_{E}\Delta\gamma_0/^\circ$	180	180
	$\gamma_0^{min}/^\circ$	0, 90	0, 90
	$\gamma_0^{max}/^\circ$	50, 130	50, 130
P2A	ΔE/kJ mol^{-1}	459	150
	$_{E}\Delta\gamma_0/^\circ$	180	180
	$\gamma_0^{min}/^\circ$	0	0
	$\gamma_0^{max}/^\circ$	90	90
P2B	ΔE/kJ mol^{-1}	459	150
	$_{E}\Delta\gamma_0/^\circ$	180	180
	$\gamma_0^{min}/^\circ$	0	0
	$\gamma_0^{max}/^\circ$	90	90
	$_{\gamma}\Delta\gamma_0/^\circ$	180	180
	$_{max}\Delta\gamma_i/^\circ$	9	20
P3	ΔE/kJ mol^{-1}	258	72
	$_{E}\Delta\gamma_0/^\circ$	180	180
	$\gamma_0^{min}/^\circ$	0	0
	$\gamma_0^{max}/^\circ$	90	90
	$_{\gamma}\Delta\gamma_0/^\circ$	180	180
	$_{max}\Delta\gamma_i/^\circ$	9 $(i = 1-6)$ 360 $(i = 15, 16)$	20 $(i = 1-6)$ 360 $(i = 15, 16)$
T1A	ΔE/kJ mol^{-1}	48	26
	$_{E}\Delta\gamma_0/^\circ$	180	180
	$\gamma_0^{min}/^\circ$	170	0
	$\gamma_0^{max}/^\circ$	90	110
T1B	ΔE/kJ mol^{-1}	50	26
	$_{E}\Delta\gamma_0/^\circ$	180	180
	$\gamma_0^{min}/^\circ$	170	5
	$\gamma_0^{max}/^\circ$	90	110
	$_{\gamma}\Delta\gamma_0/^\circ$	180	180
	$_{max}\Delta\gamma_i/^\circ$	5	7

TABLE 3 *continued*

model		*HHL*	*WCMP*
T2A	$\Delta E/\mathrm{kJ\ mol^{-1}}$	25	12
	${}_{E}\Delta\gamma_0/^\circ$	180	180
	$\gamma_0^{min}/^\circ$	160	0
	$\gamma_0^{max}/^\circ$	60	80
T2B	$\Delta E/\mathrm{kJ\ mol^{-1}}$	25	11
	${}_{E}\Delta\gamma_0/^\circ$	180	180
	$\gamma_0^{min}/^\circ$	160	5
	$\gamma_0^{max}/^\circ$	60	80
	${}_{\gamma}\Delta\gamma_0/^\circ$	180	180
	${}_{max}\Delta\gamma_i/^\circ$	2	1.5

a critical assessment of the extent to which the results from these computational investigations can be compared with experimental results on the dynamic properties of urea molecules in solids.

3.1. Pure Urea Structure

3.1.1. Models of type P1

For model P1A, in which the first shell is included in the cluster as a fixed shell, the graph (Fig. 3) of $E(\gamma_0)$ *versus* γ_0 has minima at $\gamma_0 = n \times 90^\circ$ (n = integer). The rotation barrier is 20.7 kJ mol^{-1} for the HHL potential and 11.9 kJ mol^{-1} for the WCMP potential.

For model P1B, in which the molecules of the first shell are allowed to reorient, the energy minimization at $\gamma_0 = 0^\circ$ using the experimental crystal structure as the starting point produced a structure very different from the experimental crystal structure for both the HHL and WCMP potentials; specifically, some of the atoms of molecules in the first shell that would normally from hydrogen bonds to molecules of the second shell (which is absent in this model) reorient substantially in order to from hydrogen bonds to other molecules *within* the first shell. These observations suggest that the cluster used in model P1B is not sufficiently large to reproduce the properties of the corresponding cluster in the crystal structure. Our investigations of larger clusters representing the pure urea structure are now discussed.

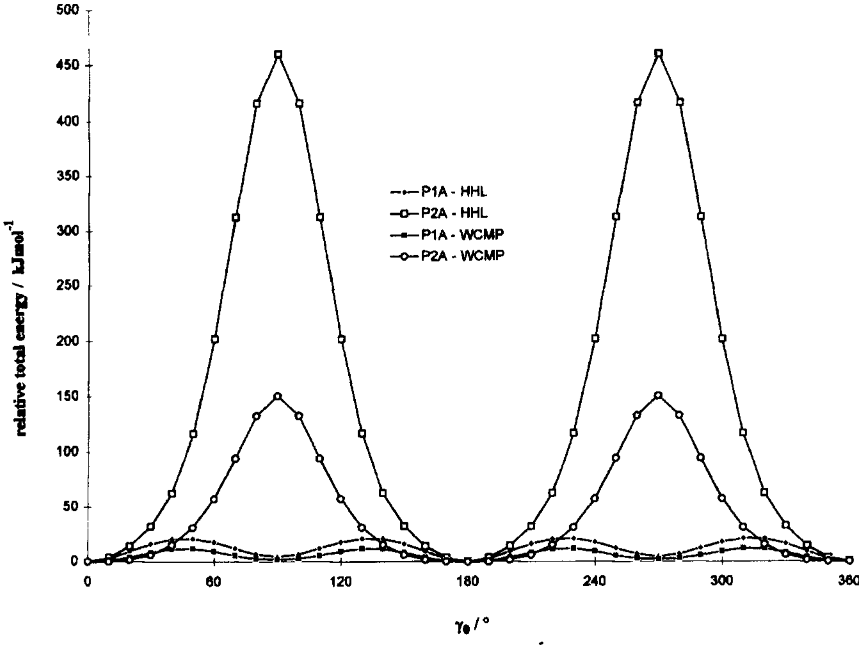

FIGURE 3 Graphs of E(γ_0) *versus* γ_0 for models P1A and P2A computed using the HHL and WCMP potentials.

3.1.2. Models of type P2

In model P2A (Fig. 3), in which both first and second shells are included as fixed shells, the energy increases significantly around $\gamma_0 = 90°$. Inspection of the structure shows that the nitrogen atoms of the central urea molecule approach close (N...N distance 2.44 Å at $\gamma_0 = 90°$) to nitrogen atoms of molecules 15 and 16 of the fixed second shell. This suggests (*vide infra*) that, in the real system, molecules 15 and 16 will reorient (i.e. γ_{15} and γ_{16} will deviate from 0°) when γ_0 approaches 90° in order to eliminate this close approach (and the associated repulsive interaction) between NH_2 groups of the central urea molecule and NH_2 groups of molecules 15 and 16.

In model P2B, the first shell of molecules (only) is allowed to relax in the energy minimization with the second shell of molecules fixed. Note that, for this model, the optimum structure of the cluster at $\gamma_0 = 0°$ reproduces well the geometry of the corresponding cluster in the experimental crystal structure. As a consequence of the strong repulsive interaction evident from model P2A between the central urea molecule and molecules of the fixed second shell, it is not surprising that similar rotation barriers are obtained for model P2B (in which the second shell is also fixed) and model P2A. For this reason, it was considered necessary to allow some molecules of the second shell to relax in order to give a realistic description of the dynamic properties.

However, when all the molecules of the first and second shells were allowed to relax in the energy minimization calculation (model P2C), problems analogous to those described above for model P1B were encountered, with the minimum energy configuration at $\gamma_o = 0^\circ$ not reproducing the experimental crystal structure.

3.1.3. *Model P3*

In model P3, molecules of the first shell plus molecules 15 and 16 in the second shell were allowed to relax in the energy minimization calculation (model P3), with all other molecules in the second shell fixed. In order to provide a more correct representation of the environment around molecules 15 and 16 in the crystal structure, two molecules (denoted 25 and 26 – see Fig. 1) from the third shell were added to form hydrogen bonds to hydrogen atoms of molecules 15 and 16. For both the HHL and WCMP potentials, the graph of $E(\gamma_0)$ *versus* γ_0 (Fig. 4) has a periodicity of 180° and the repulsion at $\gamma_0 = 90^\circ$ is still significant.

For the HHL potential, graphs of γ_i *versus* γ_0 show identical behaviour for molecules 3 and 4 and identical behaviour for molecules 5 and 6 (these pairs of molecules are related by the symmetry of the cluster). As shown in Figure 5, there are abrupt changes (109°) in γ_{15} and γ_{16} between $\gamma_0 = 90^\circ$ and 100° and between $\gamma_0 = 270^\circ$ and 280°, implying that jumps of molecules 15 and 16 are directly correlated to reorientation of the central urea molecule. Note that, at $\gamma_0 = 180^\circ$, γ_{15} and γ_{16} are also equal to 180°, and complete rotation of molecules 15 and 16 in response to rotation of the central urea molecule is clearly implicated.

For the WCMP potential, the behaviour is very similar to that described above for the HHL potential. Abrupt changes (112°) in γ_{15} and γ_{16} are observed $\gamma_0 = 90^\circ$ and 100° and between $\gamma_0 = 270^\circ$ and 280° and $\gamma_{15} = \gamma_{16} = 180^\circ$ at $\gamma_0 = 180^\circ$. Thus, the WCMP potential also suggests that molecules 15 and 16 undergo complete rotation in response to rotation of the central urea molecule.

3.2. Urea Tunnel Structure

3.2.1. *Models of type T1*

For model T1A, the graphs of $E(\gamma_0)$ *versus* γ_0 computed using the HHL and WCMP potentials are similar and exhibit a periodicity of 180°; these graphs

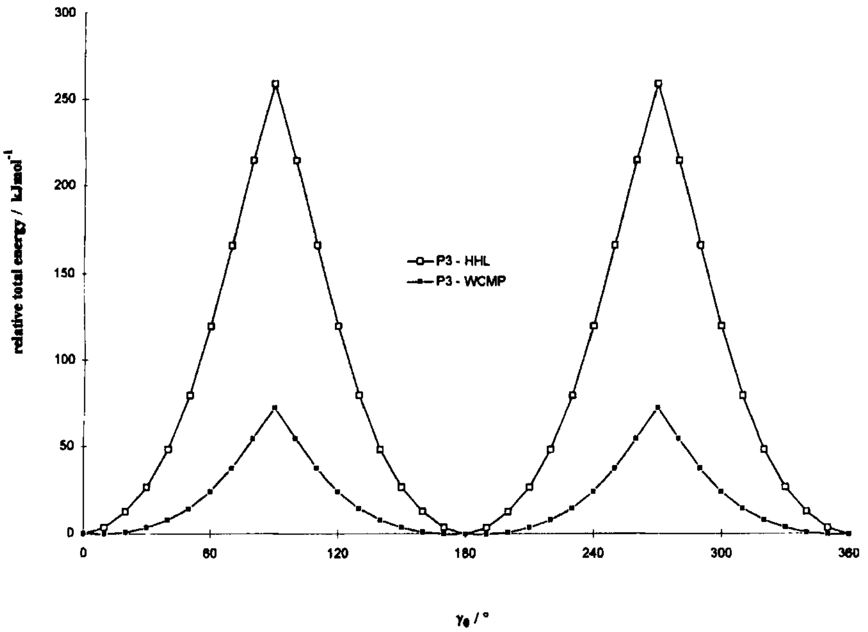

FIGURE 4 Graphs of $E(\gamma_0)$ *versus* γ_0 for model P3 computed using the HHL and WCMP potentials.

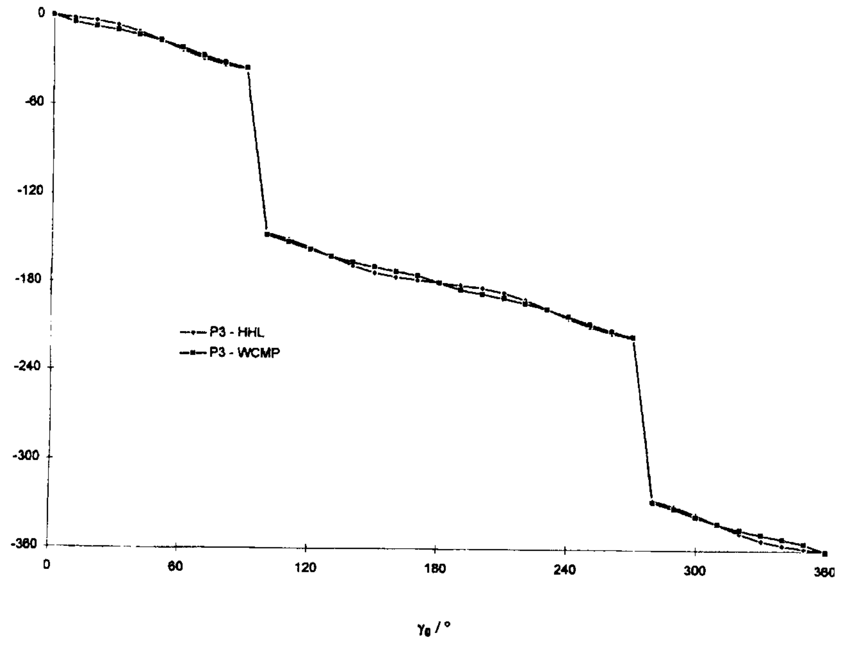

FIGURE 5 Graphs of γ_{15} and γ_{16} *versus* γ_0 for model P3 computed using the HHL and WCMP potentials.

have minima at $\gamma_0 = 170°$ and $350°$ (HHL) and $\gamma_0 = 0°$ and $180°$ (WCMP), and maxima at $\gamma_0 = 90°$ and $270°$ (HHL) and $\gamma_0 = 110°$ and $290°$ (WCMP). The rotation barrier is 48 kJ mol^{-1} for the HHL potential and 26 kJ mol^{-1} for the WCMP potential.

For model T1B, in which the molecules of the first shell are allowed to relax, the initial configuration $\{\gamma_i = 0°: i = 0, 1, \ldots, 6\}$ corresponding to the experimental crystal structure is stable upon energy minimization, and the resulting structure is close to the corresponding cluster in the crystal structure. The graph of $E(\gamma_0)$ *versus* γ_0 (Fig. 6) has periodicity of 180° in γ_0, as a consequence of the 2-fold symmetry axis of the cluster coincident with the C=O bond of the central urea molecule. The energy barriers for rotation of the central urea molecules are 50 kJ mol^{-1} (HHL) and 26 kJ mol^{-1} (WCMP). Graphs of γ_i *versus* γ_0 have a periodicity of 180° in γ_0; as a consequence of the symmetry of the cluster, the behaviour of molecules 1 and 2 is identical, the behaviour of molecules 3 and 4 is identical, and the behaviour of molecules 5 and 6 is identical. The fluctuations in the rotation angles of the molecules in the first shell (in response to the rotation of the central urea molecule) are small (less than *ca.* 5° (HHL) and *ca.* 7° (WCMP)), and the geometry of the cluster remains close to that of the experimental crystal structure throughout the rotation of the central urea molecule.

3.2.2. *Models of type T2*

Comparing models T2A and T1A, the energy barrier for rotation of the central urea molecule is lower for model T2A (25 kJ mol^{-1} (HHL); 12 kJ mol^{-1} (WCMP)) than for model T1A (48 kJ mol^{-1} (HHL); 26 kJ mol^{-1} (WCMP)), suggesting that the rotation is stabilized by the presence of the second shell. The graphs of $E(\gamma_0)$ *versus* γ_0 for model T2A have minima at $\gamma_0 = 160°$ and $340°$ (HHL) and $\gamma_0 = 0°$ and $180°$ (WCMP), and maxima at $\gamma_0 = 60°$ and $240°$ (HHL) and $\gamma_0 = 80°$ and $260°$ (WCMP).

For model T2B, in which both first and second shells are present, but only the molecules of the first shell are allowed to relax, the initial configuration corresponding to the crystal structure remains stable upon energy minimization (i.e. the geometry of the resulting optimum configuration is close to the experimental crystal structure). The graphs of $E(\gamma_0)$ *versus* γ_0 (Fig. 6) have periodicity of 180° in γ_0 for both potentials, although they differ significantly in shape and in the energy barrier (25 kJ mol^{-1} (HHL) and 11 kJ mol^{-1} (WCMP)) for rotation of the central urea molecule. The rotation angles of the molecules in the first shell exhibit only small fluctuations (less than *ca.* 2° (HHL) and less than *ca.* 1.5° (WCMP)) as the central urea molecule is rotated.

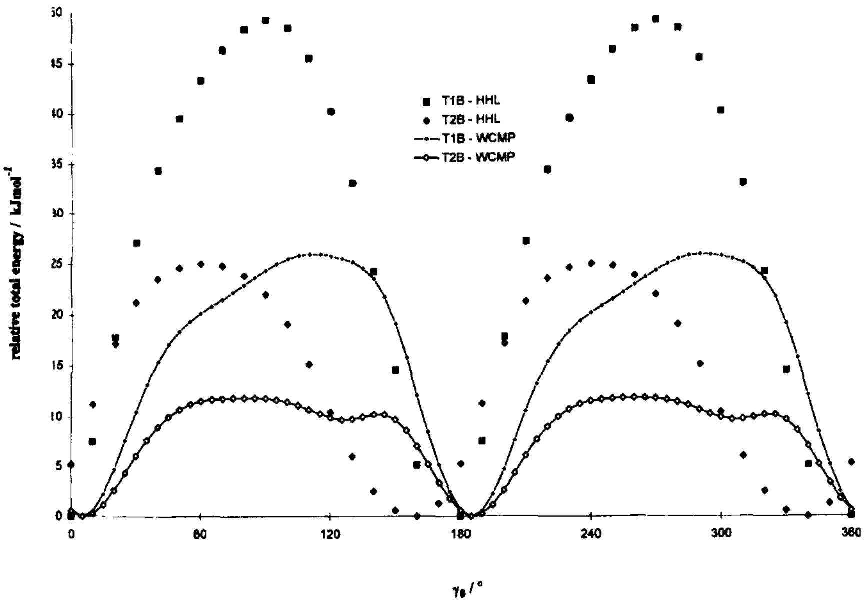

FIGURE 6 Graphs of $E(\gamma_0)$ *versus* γ_0 for models T1B and T2B computed using the HHL and WCMP potentials.

Molecules 1 and 2 behave in an identical manner, molecules 3 and 4 behave in an identical manner, and molecules 5 and 6 behave in an identical manner.

4. DISCUSSION

The application of the computational approaches described above to investigate the dynamics of urea molecules in the pure urea structure and the urea tunnel structure has raised several important issues.

For the pure urea structure, the use of a cluster representation is limited by the fact that the geometry of the cluster taken from the experimental crystal structure is unstable under structural relaxation of all non-central urea molecules in the cluster. Thus, models P1B and P2C do not provide an adequate representation of the experimental system as, in each case, the optimum configuration at $\gamma_0 = 0°$ differs significantly from the experimental crystal structure. In model P2B, in which the second shell of molecules is kept fixed but the first shell is allowed to relax, the system is probably too constrained to yield unambiguous information on whether the motions of different urea molecules are correlated. These problems could be overcome by considering a cluster that is sufficiently large to ensure that the relaxed configuration at $\gamma_o = 0^\circ$ is close to the experimental crystal structure; however, it was not feasible to consider larger clusters within the present work due to the excessive computational time required. Alternatively, it would be interesting to consider a model in which the outer shell of urea molecules is subject to constraints intermediate between those applied in model P2B (i.e. molecules fixed) and model P2C (i.e. no constraints).

As the relaxed cluster at $\gamma_o = 0^\circ$ reproduces the experimental crystal structure under the constraints of models P2B and P3, we focus our discussion of the pure urea structure on the results obtained for these models. For these models, some (model P3) or all (model P2B) of the urea molecules in the second shell were kept fixed, thus exerting a constraint on the relaxation of the first shell. It is not clear whether this represents an adequate approximation to the experimental situation, in which interaction of the second shell with outer (i.e. third, fourth, etc) shells will indeed, *on a time average*, maintain $\gamma_i = 0^\circ$ for all molecules in the second shell. However, as a result of the fixed second shell of molecules, model P2B cannot exhibit correlated motions between molecules in the first and second shells, and, if such correlations do exist in practice, this model cannot adequately reflect the dynamic behaviour of the real system. In the computed trajectory for model P2B, rotation of the central urea molecule is not associated with any significant reorientation of the molecules in the first shell, and the rotation barrier is essentially the same as the rotation barrier for model P2A (in which all molecules in the first and second shells are fixed). Thus, the rotation barrier is not lowered by allowing the molecules in the first shell (and only these molecules) to relax. As the central urea molecule is rotated away from $\gamma_0 = 0^\circ$, the hydrogen bonds that it forms with molecules 3 and 4 (see Fig. 1) are broken, whereas the N—H...O=C distances for the other hydrogen bonds are not changed (although clearly the angular characteristics of these other hydrogen bonds do change as the central urea molecule is rotated). However, as the central urea molecule approaches $\gamma_o = 90^\circ$, two new hydrogen bonds are formed (Fig. 7) between the N—H hydrogen atoms of the central urea molecule and the oxygen atoms of molecules 5 and 6. The formation of these new hydrogen bonds during rotation of the central urea molecule undoubtedly serves to lower the rotation barrier for the central urea molecule. Molecules 5 and 6 (in the orientaions with $\gamma_5 \approx 0^\circ$ and $\gamma_6 \approx 0^\circ$) already from hydrogen bonds (involving an N—H group from each molecule) with the oxygen atom of the central urea molecule, and if molecules 5 and 6 were to rotate simultaneously with the central urea molecule, this hydrogen bonding would be lost. Thus it is probable that rotation of a given molecule

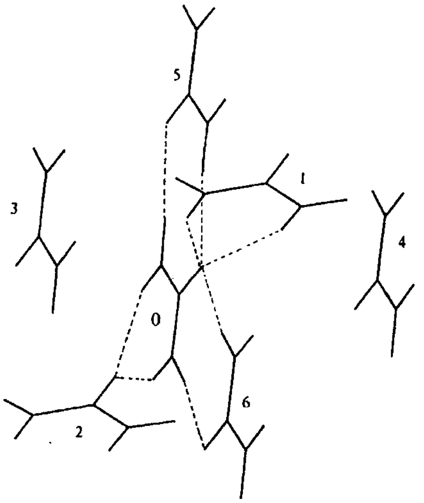

FIGURE 7 Illustration of the formation of new hydrogen bonds between the central urea molecule and neighbouring molecules 5 and 6 in the pure urea structure when the orientation of the central urea molecule is $\gamma_0 = 90°$.

(the central urea molecule in this case) may actually require that two of its neighbours (molecules 5 and 6 in this case) remain in the orientations that they adopt in the average crystal structure. This would suggest that rotation of a given urea molecule by 180° (i.e. the motion inferred from ^{2}H NMR spectroscopy) should not occur simultaneously with 180° jumps of these two neighbouring urea molecules.

In model P3, urea molecules 15 and 16 undergo complete rotation as the central urea molecule is rotated by 180°, and undergo significant jumps ($\Delta\gamma_{15} \approx \Delta\gamma_{16} \approx 110°$) at specific values of the rotation angle of the central urea molecule. There is clearly a significant degree of correlation between the dynamics of urea molecules 15 and 16 and the central urea molecule.

For the pure urea structure (for either the HHL or WCMP potentials), none of the computed rotation barriers is in close agreement with the rotation barriers derived from experimental data. This is probably a reflection both of inadequacies in the potential energy parameterizations used for representing the energetic properties of structures far from equilibrium (see the discussion below), and of inadequacies (discussed above) of the cluster representation of the pure urea structure.

For the urea tunnel structure, direct comparison of the computed and experimental results should be carried out with caution, as the system investigated computationally is hypothetical (the urea tunnel structure considered in our calculations does not contain guest molecules). Nevertheless, it is noteworthy that the rotation barrier (25 kJ mol^{-1}) computed using the HHL potential for the empty urea tunnel structure is very close to the experimental rotation barrier (23 kJ mol^{-1}) for nonadecane/urea. However, as the present results do not allow an assessment of the extent to which host-guest interaction influences the rotation barrier, we make no attempt to draw further conclusions from this observation.

For the urea tunnel structure, the results are virtually independent of the number of structural variables in the calculation (i.e. the number of neighbouring molecules allowed to relax), and it is apparent that rotation of the central urea molecule in the urea tunnel structure does not significantly affect the behaviour of the neighbouring urea molecules (with only small fluctuations in the rotation angles of the neighbouring urea molecules associated with complete rotation of the central urea molecule). In all of these aspects, the dynamic properties of the urea molecules in the urea tunnel structure differ markedly from the pure urea structure. It is interesting to consider whether the presence of guest molecules in the tunnels may influence the motion of the urea molecules, and indeed whether the presence of guest molecules may induce correlation of the motions of different urea molecules indirectly *via* host-guest interaction. Future work in this area will require careful consideration of how best to handle the incommensurate relationship between the host and guest components that is a characteristic of most urea inclusion compounds.

We now compare the two potential energy parameterizations considered in this work. Initially, we recall (from Section 2.2) that both parameterizations provide good representations of the (bulk) experimental crystal structure. The HHL and WCMP potentials differ fundamentally in the approach for considering the electrostatic interaction. The HHL potential uses an empirical point charge model, derived by fitting the parameters of the potential against experimental crystal structures for a series of amides. The WCMP potential, on the other hand, uses the more complex description of the charge distribution provided by distributed multipole analysis of the SCF wavefunction determined from *ab initio* calculation for the urea molecule, and therefore has a stronger theoretical foundation. It is clear that properties that are dominated by long range interaction should be better represented by the WCMP potential. The HHL and WCMP potentials also differ in the approach for considering the repulsion interaction, with an Ar^{-12} term used for all atoms except hydrogen in the HHL potential and an Aexp(-Br) term used for all atoms in the WCMP potential.

For the pure urea structure, the shapes of the $E(\gamma_0)$ *versus* γ_0 graphs for a given model are similar for the HHL and WCMP potentials, although the energy barriers are significantly higher for the HHL potential. The dynamic trajectories (assessed from the variations in the rotation angles γ_i as the central urea molecule is rotated) obtained for a given model using the HHL and WCMP potentials are also substantially similar, although the fluctuations in the rotation angles γ_i are generally larger for the WCMP potential. It is clear that the energy barrier and dynamic trajectory for rotation of the central urea molecule is influenced largely by the repulsion interaction, and both the HHL and WCMP potentials give an adequate representation (at least at a qualitative level) of the interactions at short range. Nevertheless, the differences in the ways in which the HHL and WCMP potentials represent the repulsion interaction are clearly manifested in the differences in the results (particularly the energy barriers) obtained. It is relevant to note that the parameters describing repulsion within the HHL and WCMP potentials were derived from fitting equilibrium crystal structures, and that such parameters are not necessarily optimum for describing systems far from equilibrium (such as at an intermediate stage within a dynamic trajectory). For this reason, the discrepancies between the energy barriers obtained for the HHL and WCMP potentials are perhaps not surprising, and better agreement is probably beyond the level at which repulsion is currently handled within these potential energy parameterizations. The future development of a more realistic and specific repulsion potential should also assess the extent to which the geometry of the molecule becomes distorted, during the dynamic process, as a consequence of the repulsive intermolecular interactions.

For the urea tunnel structure, the energy barriers computed for a given model using the HHL and WCMP potentials are generally in better agreement than for the pure urea structure, although there are significant differences in the shapes of the $E(\gamma_o)$ *versus* γ_o graphs (Fig. 6). It is clear that the energy barrier and dynamic trajectory for rotation of the central urea molecule are influenced primarily by the loss of hydrogen bonding (as the NH_2 groups of the central urea molecule protrude into the tunnel) and not by the establishment of specific repulsive interactions with neighbouring urea molecules. Differences in the results obtained for the HHL and WCMP potentials presumably reflect differences in the way in which these parameterizations represent structures far from equilibrium, and may originate in the electrostatic part of the potential. For the urea tunnel structure there are only very small fluctuations in the rotation angles γ_i as a function of rotation of the central urea molecule, and in this regard similar behaviour is predicted by both the HHL and WCMP potentials.

With regard to the stability of the clusters representing the experimental crystal structure (i.e. relaxation with $\gamma_o = 0°$), both potentials give the same results. As discussed previously, for models in which *all molecules* in the clusters are allowed to relax, the cluster representing the urea tunnel structure (model T1B) is stable whereas the clusters representing the pure urea structure (models P1B and P2C) are unstable. Clearly it is relevant to consider what size of cluster is required for the pure urea structure to represent closely the behaviour of the bulk crystal structure. The cluster size also has important implications with regard to probing the extent of correlations of the motions of different urea molecules. For the pure urea structure, we have shown that the rotation of a urea molecule requires some correlation with the motions of specific molecules (15 and 16) in the second shell in order to avoid strong repulsive interactions; in order to investigate the spatial extent of these correlated motions (i.e. the size of the region in the crystal over which the motions are correlated), it is clearly necessary to consider clusters larger than those investigated here.

Acknowledgements

We are grateful to University College London and the University of Birmingham (studentships to SC), EPSRC (general support to KDMH and SLP) and the Nuffield Foundation (Science Research Fellowship to KDMH). We thank Mr David Coombes, Mr Rob Apaya and Dr Ashley George for computational assistance.

References

[1] Wyckoff, R. W. G. and Corey, R. B. (1934). "Spectrometric measurements on hexamethylene tetramine and urea", *Z. Krist.*, **89**, 462.

[2] Vaughan, P. and Donohue, J. (1952). "The structure of urea. Interatomic distances and resonance in urea and related compounds", *Acta Cryst.*, **5**, 530 [see also: Caron, A. J. Donohue (1969) "Redetermination of thermal motion and interatomic distances in urea", *Acta Cryst.*, **B25**, 404

[3] Smith, A. E. (1952). "The crystal structure of the urea-hydrocarbon complexes", *Acta Cryst.*, **5**, 224.

[4] Harris, K. D. M. and Thomas, J. M. (1990). "Structural aspects of urea inclusion compounds and their investigation by X-ray diffraction: a general discussion", *J. Chem. Soc., Faraday Trans.*, **86**, 2985.

[5] Takemoto, K. and Sonoda, N. (1984). "Inclusion compounds of urea, thiourea and selenourea", in *Inclusion Compounds* [Eds: J. L. Atwood, J. E. D. Davies, D. D. MacNicol], **2**, Academic Press, New York, p. 47

[6] Hollingsworth, M. D. and Harris, K. D. M. (1996). "Urea, thiourea and selenourea", in *Comprehensive Supramolecular Chemistry* [Eds: R. Bishop, D. D. MacNicol, F. Toda], **6**, Pergamon Press, Oxford, p. 177.

[7] Harris, K. D. M (1993). "Molecular confinement", *Chemistry in Britain*, **29**, 132.

[8] Harris, K. D. M. (1993). "Investigating the structure and dynamics of a family of organic solids: the alkane/urea inclusion compounds", *J. Solid State Chem.*, **106**, 83.

[9] Emsley, J. W. and Smith, J. A. S (1961). "Molecular motion in thiourea and urea", *Trans. Faraday Soc.*, **57**, 1233.

[10] Chiba, T. (1965). "A deuteron magnetic resonance study of urea-d_4", *Bull. Chem. Soc. Japan*, **38**, 259.

[11] Zussman, A. (1973). "Effect of molecular reorientations in urea on the ^{14}N PNQR linewidth and relaxation time," *J. Chem. Phys.*, **58**, 1514.

[12] Das, T. P. (1957). "Tunneling through high periodic barriers. II. Application to nuclear magnetic resonance in solids" *J. Chem. Phys.*, **27**, 763 [see also: Das, T. P. (1961) Erratum, *J. Chem. Phys.*, **35**, 1897].

[13] Heaton, N. J., Vold, R. L. and Vold, R. R. (1989). "Deuterium quadrupole echo study of urea motion in urea/*n*-alkane inclusion compounds," *J. Am. Chem. Soc.*, **111**, 3211.

[14] Aliev, A. E., Smart, S. P. and Harris, K. D. M. (1994). "Dynamic properties of the urea molecules in α, ω-dibromoalkane/urea inclusion compounds investigated by ^{2}H NMR spectroscopy," *J. Mater. Chem.*, **4**, 35.

[15] Guillaume, F., Sourisseau, C. and Dianoux, A. -J. (1991). "Rotational and translational motions of *n*-nonadecane in the urea inclusion compound as evidenced by incoherent quasielastic neutron scattering," *J. Chim. Phys. (Paris)*, **88**, 1721.

[16] Guillaume, F., Smart, S. P., Harris, K. D. M. and Dianoux, A. -J. (1994). "Neutron scattering investigations of guest molecular dynamics in α, ω-dibromoalkane-urea inclusion compounds," *J. Phys.: Condens. Matter*, **6**, 2169.

[17] Harris, K. D. M., Guillaume, F., Smart, S. P., Sourisseau, C. and Dianoux, A. J. (1992). "Neutron scattering investigation of host molecular motion in the hexadecane-urea inclusion compound," *J. Chem. Research*, 276.

[18] Guth, H., Heger, G., Klein, S., Treutmann, W. and Scheringer, C. (1980). "Strukturverfeinerung von Harnstoff mit Neutronenbeugungsdaten bei 60, 123 und 293 K und X-N- und X-X ($1s^2$)-Synthesen bei etwa 100 K," *Zeit. Kristall.*, **153**, 237.

[19] Price, S. L. and Stone, A. J. (1987). "The electrostatic interactions in van der Waals complexes involving aromatic molecules," *J. Chem. Phys.*, **86**, 2859.

[20] Hagler, A. T., Huler, E. and Lifson, S. (1974). "Energy functions for peptides and proteins. I. Derivation of a consistent force field including the hydrogen bond from amide crystals," *J. Am. Chem. Soc.*, **96**, 5319.

[21] Stone, A. J. (1981). "Distributed multipole analysis or how to describe a molecular charge distribution," *Chem. Phys. Lett.*, **83**, 233.

[22] Stone, A. J. and Alderton, M. (1985). "Distributed multipole analysis. Methods and applications," *Mol. Phys.*, **56**, 1047.

[23] Coombes, D. S. (1996). "Deriving intermolecular potentials for predicting the crystal structures of polar molecules," *Phil. Mag. B.* **73**, 117.

[24] Williams, D. E. and Cox, S. R. (1984). "Nonbonded potentials for azahydrocarbons: the importance of the coulombic interaction," *Acta Cryst.*, **B40**, 404.

[25] Cox, S. R., Hsu, L. H. and Williams, D. E. (1981). "Nonbonded potential function models for crystalline oxohydrocarbons," *Acta Cryst.*, **A37**, 293.

[26] Mitchell, J. B. O. and Price, S. L. (1990). "The nature of the N—H···O=C hydrogen bond: an intermolecular perturbation theory study of the formamide/formaldehyde complex," *J. Comp. Chem.*, **11**, 1217.

[27] CADPAC5: The Cambridge analytical derivatives package issue 5, Cambridge 1992. A suite of quantum chemistry programs developed by Amos, R. D. with contributions from Alberts, I. L., Andrews, J. S., Colwell, S. M., Handy, N. C., Jayatilaka, D., Knowles, P. J., Kobayashi, R., Koga, N., Laidig, K. E., Maslen, P. E., Murray, C. W., Rice, J. E., Sanz, J., Simandiras, R., Stone, A. J., Su, M. D.

[28] Price, S. L., Andrews, J. S., Murray, C. W. and Amos, R. D. (1992). "The effect of basis set and electron correlation on the predicted electrostatic interactions of peptides," *J. Am. Chem. Soc.*, **114**, 8268.

[29] Spackman, M. A., Weber, H. P. and Craven, B. M. (1988). "Energies of molecular interactions from Bragg diffraction data," *J. Am. Chem. Soc.*, **110**, 775.